Distinguishing cells by their first-order transient motion response under an optically induced dielectrophoretic force field

Zhao, Yuliang; Liang, Wenfeng; Zhang, Guanglie; Mai, John D.; Liu, Lianqing; Lee, Gwo-Bin; Li, Wen J.

Published in:
Applied Physics Letters

Published: 28/10/2013

Document Version:
Final Published version, also known as Publisher's PDF, Publisher's Final version or Version of Record

Published version (DOI):
10.1063/1.4827300

Publication details:
Zhao, Y., Liang, W., Zhang, G., Mai, J. D., Liu, L., Lee, G.-B., & Li, W. J. (2013). Distinguishing cells by their first-order transient motion response under an optically induced dielectrophoretic force field. *Applied Physics Letters*, *103*(18), Article 183702. https://doi.org/10.1063/1.4827300

Applied Physics Letters

Distinguishing cells by their first-order transient motion response under an optically induced dielectrophoretic force field

Cite as: Appl. Phys. Lett. **103**, 183702 (2013); https://doi.org/10.1063/1.4827300
Submitted: 09 August 2013 • Accepted: 11 October 2013 • Published Online: 28 October 2013

Yuliang Zhao, Wenfeng Liang, Guanglie Zhang, et al.

Distinguishing cells by their first-order transient motion response under an optically induced dielectrophoretic force field

Yuliang Zhao,[1] Wenfeng Liang,[1,2] Guanglie Zhang,[1,a)] John D. Mai,[1] Lianqing Liu,[2] Gwo-Bin Lee,[3] and Wen J. Li[1,2,b)]
[1]*Department of Mechanical and Biomedical Engineering, City University of Hong Kong, Kowloon, Hong Kong*
[2]*State Key Laboratory of Robotics, Shenyang Institute of Automation, Chinese Academy of Sciences, Shenyang, China*
[3]*Department of Power Mechanical Engineering, National Tsing Hua University, Hsinchu, Taiwan*

(Received 9 August 2013; accepted 11 October 2013; published online 28 October 2013)

This letter reports our characterization of the transient motion of cells under an optically induced dielectrophoresis (ODEP) force field. Different types of human cells repeatably undergo a first-order transient motion response when subjected to a specific ODEP force field. A kernel function is derived to describe this transient motion. This function can be generally matched to experimental data for Raji cells and red blood cells by measuring two parameters: the initial velocity and the transient time-constant. They are uniquely different for Raji cells and RBCs. Support vector machine is used to distinguish between them based on their transient response characteristics.
 [http://dx.doi.org/10.1063/1.4827300]

Using digitally and optically projected images to define "virtual" electrodes, optically induced dielectrophoresis (ODEP)[1–3] enables simplified, real-time manipulation of micro particles, as compared to the metal electrodes based dielectrophoresis (DEP) platforms. Precisely controlled actions, such as the transport, separation, assembly, and focusing of micro particles, have been commonly reported using the ODEP mechanism. However, little attention has been given to the complete analysis of the continuous motion of these micro particles. Most research into DEP/ODEP has only focused on simulations[4,5] and experiments,[6,7] where the motion of a particle was always simplified by assuming a uniform linear velocity or a critical state, where the ODEP force is balanced by the fluidic drag force on the particle.[8–11] The lack of a complete, dynamic description of the forces affecting particle motion limits the accuracy of applying ODEP in a quantitative manner. Due to the extremely fast time-constant for the initial acceleration (i.e., $\sim 10^{-6}$ s) of micron-scale particles in the presence of a DEP force field, classical theory describes the DEP force acting on a biological cell as only a linear function of the cellular velocity. The acceleration of a cell when a DEP force is exerted on it has been neglected in the past, due to the inability of the human eye to "capture" this motion when observing a cell under an optical microscope.

In this letter, the motion of a particle under the influence of an ODEP electric-field is theoretically derived and experimentally verified by using a computer-vision algorithm. Researchers generally agree that the magnitude of DEP force is proportional to the resulting particle velocity. We present here an analysis that yields another set of equations for particle motion under a DEP force field. Furthermore, these equations are verified via experiments where the motion of Raji cells and red blood cells (RBCs) are observed in the presence of a negative ODEP force. High resolution video from a microscope system is used to record the cell motion, and a particle tracking software[12] is applied to analyze the results. The experimental results confirm the theoretical model. Moreover, these motion equations also reveal more information, such as the distribution of the ODEP force, a transient time constant for the motion, and the response characteristics of different cell types.

Fig. 1(a) shows a schematic illustration of the ODEP system, and Fig. 1(b) shows an image of cell repelled away from the light beam in the ODEP chip. Fig. 1(c) depicts the geometrical configuration of the ODEP chip, which comprised a 1 μm thick layer of hydrogenated amorphous silicon (a-Si:H) deposited on an indium tin oxide (ITO)-coated glass substrate, the liquid chamber, and the ITO glass layer. The medium with a relative permittivity of 80 and a conductivity of 1.3×10^{-2} S/m is loaded between the two glass substrates. An AC voltage bias is applied between the two ITO layers. When a digital image is projected onto the surface of the a-Si:H layer, virtual electrodes are formed on the illuminated area due to a local increase in electrical conductivity of a-Si:H. Similar to a metal electrode, a non-uniform electric field is induced, which generates the DEP force and enables the manipulation of the micro-particles.

Besides the DEP force and the drag force, several other forces arise when cells move in an ODEP chip. Buoyancy, gravitational forces, thermal effects, electro-osmosis, Brownian motion, and particle-to-particle interactions have been discussed by many other researchers.[3,8] However, most of these forces can be neglected under our experimental conditions. Specifically, a typical Raji cell has a diameter of 12 μm and a RBC varies in diameter from 6.2 to 8.2 μm,[13] and the AC bias is 25 $V_{p\text{-}p}$ at 60 kHz. Of the previously mentioned forces and effects, only the gravitational force and buoyancy are on the same order of magnitude as the DEP force (10^{-12} N). The other forces have a much lower order of magnitude effect ($<10^{-15}$ N). Furthermore, the densities of these cells and the fluid medium are almost the same since

a)For computer vision algorithms contact: gl.zhang@cityu.edu.hk
b)For cell motions under influence of electrical field contact: wenjli@cityu.edu.hk

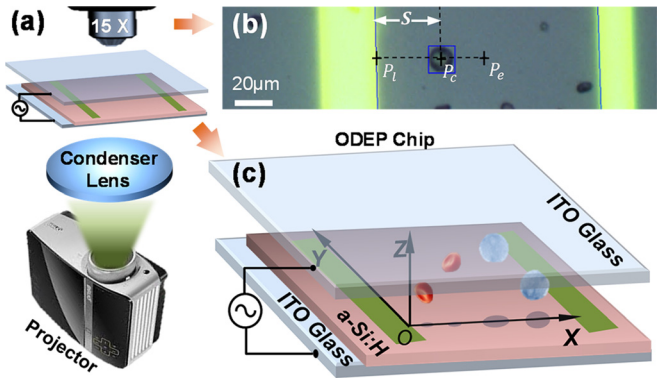

FIG. 1. Illustration showing the manipulation of RBCs and Raji cells in a fluid by a digitally generated image (green light beams) projected onto an ODEP chip. (a) The ODEP system. (b) An image of Raji cell manipulation using the ODEP system. (c) The ODEP chip.

the cells are observed to be neutrally buoyant in solution. Hence, the resultant effects of the buoyancy and gravitational forces are neglected. Thus, the initial state equation of the DEP-induced kinetics on a cell (of mass m and with a radius R) can be described as[8–11]

$$m\frac{du}{dt} = F_{DEP} + F_{Viscosity}, \tag{1}$$

where u is the velocity of the cell, F_{DEP} is the DEP force on the cell, $F_{Viscosity} = 6\pi R\eta u$, and η is the dynamic viscosity of the fluid medium. The function of the velocity is solved from Eq. (1) as

$$u(t) = \frac{F_{DEP}}{6\pi R\eta}(1 - e^{-\frac{t}{\tau_a}}), \tag{2}$$

where $\tau_a = m/(6\pi R\eta)$. Since τ_a–10^{-6} s, this means that the typical time t is too small to be observed, and hence the acceleration phase is usually neglected. So the classical equation for the particle velocity with DEP force is simplified as

$$u = \frac{F_{DEP}}{6\pi R\eta}. \tag{3}$$

This classical solution has been widely used to calculate the DEP force from the particle velocity[6,7] or to calculate the particle velocity from DEP force, although there are two major problems. The first one is that the DEP force and the particle velocity are coupled, which means one value must be known in order to calculate the other. In most laboratory situations, it is difficult to experimentally measure either value. The second problem is that this equation is a discrete function while the particle's motion is not a uniform movement. This non-uniformity makes predicting the particle trajectory difficult and inaccurate.

Based on the aforementioned problems, Eq. (1) can be modified in the following manner. Since the DEP force varies with velocity, we make an assumption that $F_{DEP} = K \times u$, where K is a scaling coefficient. Inserting this assumption back into Eq. (1) yields

$$m\frac{du}{dt} = (K + 6\pi R\eta) \times u. \tag{4}$$

The following equation can be obtained by solving this analytical expression for velocity $u(t)$ as a function of time:

$$u(t) = U_0 e^{-\frac{t}{\tau}}, \tag{5}$$

where U_0 represents the initial velocity when particles experience the largest DEP force, τ is defined as $\tau = m/(6\pi R\eta - K)$. U_0 and τ are two time-independent constants. Instead, they are dependent on the electric field and the physical properties of the particle. Now the velocity $u(t)$ only varies monotonically with t. In other words, the motion of a specific particle in a specific DEP environment can be described by a velocity function that exponentially decays with respect to time. Similar to other physical functions, τ is a time constant that can be determined by measuring the time to travel some fixed length due to an impulse input. If U_0 and τ can be calculated or measured, the entire motion equation can be solved. Taking the integral and derivative of Eq. (5) yields the displacement $s(t)$ and the acceleration $a(t)$, respectively. The displacement is further expressed as

$$s(t) = U_0\tau(1 - e^{-\frac{t}{\tau}}). \tag{6}$$

K was previously defined as a scalar coefficient and can now be expressed as $K = 6\pi R\eta - m/\tau$. Finally, the complete analytical expression for the DEP force with respect to the motion of a particle is

$$F_{DEP}(t) = \left(6\pi R\eta - \frac{m}{\tau}\right) \times U_0 e^{-\frac{t}{\tau}}. \tag{7}$$

Equation (7) is more accurate and comprehensive compared to Eq. (3). First, Eq. (7) has an extra term $-m/\tau$. Although it is a small value (10^{-6}) compared to the viscosity term $6\pi R\eta$, it makes the equation an equality and not only an approximation. The extra term $u(t) \times m/\tau$ represents an inertia force which is small enough to neglect in most cases. Note that when the expression for u or s is substituted into Eq. (7), the DEP force equation becomes a continuous function that only varies with time t or distance s.

In Eq. (7), the DEP force is independent of particle position. The distribution of the DEP force on the trajectory of a particle can be obtained by inserting Eq. (6) into Eq. (7). All the equations which describe the motion of the particle have now been expressed as a function of two constant parameters U_0 and τ.

This solution for the particle velocity $u(t) = U_0 \times e^{-t/\tau}$ together with U_0 and τ has been verified by the following experiments. Raji cells and RBCs are repelled by the negative DEP force produced by a 25 μm wide light beam projected on the ITO glasses with AC bias of $25V_{p\text{-}p}$ at 60 kHz. The video of this experiment at a 1392×1040 (pixels $\times$ pixels) resolution is taken at sampling rate of 8 frames per second. 3D Cartesian coordinate system is set up according to Fig. 1(c).

Fig. 2(a) illustrates the forces affecting a Raji cell and its resulting trajectory on the X-Z plane. The trajectory of the cell is described based on the direction and magnitude of the net force. Since the direction of the resultant force is perpendicular to the y axis, there is zero displacement in this

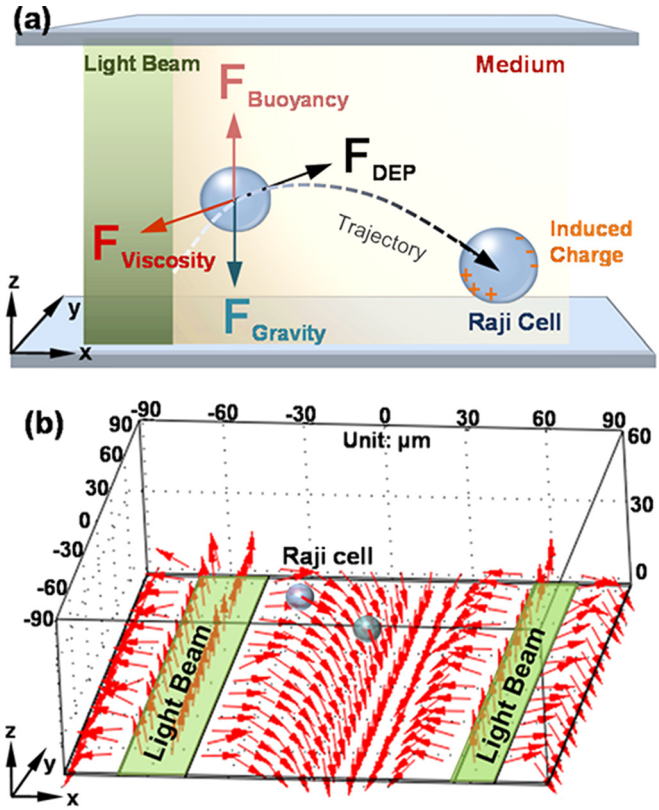

FIG. 2. Simulation of the main forces affecting the cell. (a) The force vectors on a Raji cell in the X-Z plane. (b) 3D finite element method (FEM) numerical simulation of the DEP forces on a Raji cell at the height of 6 μm from the a-Si:H surface.

direction. Along the z axis, the fluid is trapped between two glass substrates spaced 60 μm apart. The possible displacement in the z-direction is about 10 μm, but this is difficult to experimentally verify since the depth-of-field information has been lost, due to the monocular optics of the microscope. Neglecting the displacement along the z direction, the motion is simplified to a 1D linear movement along the x axis. All of the parameters discussed herein forward are the projection of the 3D vectors onto the x axis. Fig. 2(b) shows a numerical simulation of the DEP force using commercial software (Multiphysics, COMSOL AB, Sweden).

The distance s from the edge of the projected light pattern to the cell is clearly visible. By tracking a target cell and the edge of the light pattern, the distance s in each frame of video can be calculated. Fig. 3(a) shows a cell moving away from the light beam, and Fig. 3(b) shows the trajectory of the cell on X-Z plane. Combined with the elapsed time information encoded in the video, a distance-time plot (s-t plot) is produced. Fig. 3(c) gives an example of the s-t graph for a Raji cell as it moves away from the projected green line. After curve fitting, the high coefficient of determination ($r^2 = 0.993$) indicates that the data plot matches Eq. (6) well. This experimental method not only validates the theoretical analysis but also obtains two important constants U_0 and τ.

Each U_0 and τ describes a specific trajectory for a cell. By analyzing videos of 60 different Raji cells and RBC cells, their calculated trajectories are plotted. We find that 97% of these cell trajectories follow Eq. (6). Fig. 4(a) shows an s-t graph with 14 cell trajectories plotted. The coefficient of

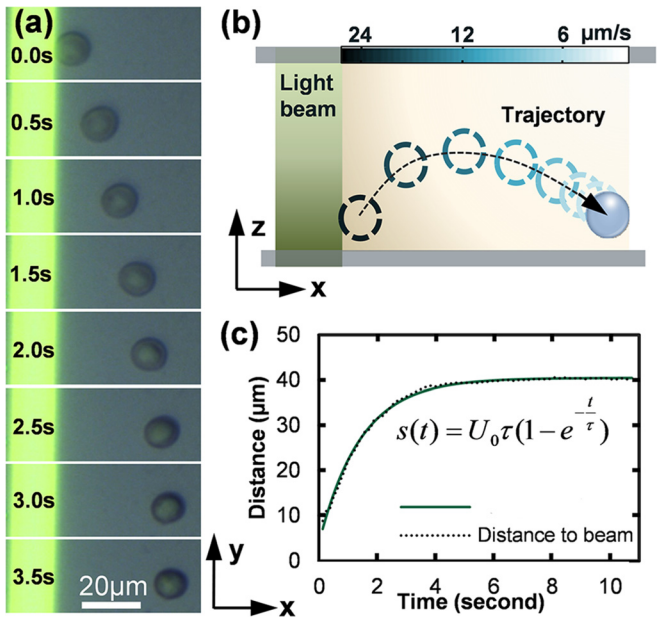

FIG. 3. (a) Time-lapsed images of one Raji cell moving away from a projected line due to a negative ODEP force. (b) The simulated trajectory based on the direction of cell movement on the X-Z plane. (c) s-t data obtained from recorded cell experiment videos and its curve fitting.

determination r^2 varies from 0.89 to 0.99 and the average r^2 fit is 0.977. 64% of the 60 cell trajectories had a r^2 fit of 0.99 or better. Taking the first and second derivatives of Eq. (6), the velocity $u(t)$ and the acceleration $a(t)$ with respect to time can both be calculated and match the trends predicted by motion equations former derived. Fig. 4(b) plots the measured distance, the calculated velocity, acceleration, and drag force as a function of time for a Raji cell.

In Eq. (6), $u(0) = U_0$. The initial velocity is at the maximum value and the initial acceleration is also at the maximum value but in the opposite direction of the velocity. This means that a cell initially experiences a negative resultant force whose magnitude decreases as the time t increases. The movement of the cell mainly depends on the DEP force and the drag force. Initially, the DEP force is larger than all the other forces. Thus, there is a quick acceleration over a short time (τ_a–10^{-6} s). After which, the velocity of the cell reaches a maximum value. Simultaneously, the resistance due to viscosity also increases to a maximum value, until it is approximately equal to the driving DEP force. This force balance causes the acceleration to quickly decrease as shown in Fig. 4(b). In Eq. (6), as time approaches $t = +\infty$, the maximum displacement becomes $s_{max} = U_0\tau$. The parameter $U_0\tau$ represents the maximum displacement of a cell, which can also be considered as the farthest effective distance that a DEP force field can have on a cell.

By further analyzing these equations, many quantifiable physical relationships can be understood. For example, characteristic values for a particle under a DEP force field can be defined, i.e., different motion of cells in the force field could be another indicator of cellular polarization, permittivity, and conductivity. These dielectric properties can lead to future approaches for the manipulation, assembly, and separation of bio-particles.

Using the calculated values for U_0 and τ from the experiments with Raji cells and RBCs, Fig. 4(c) shows that it

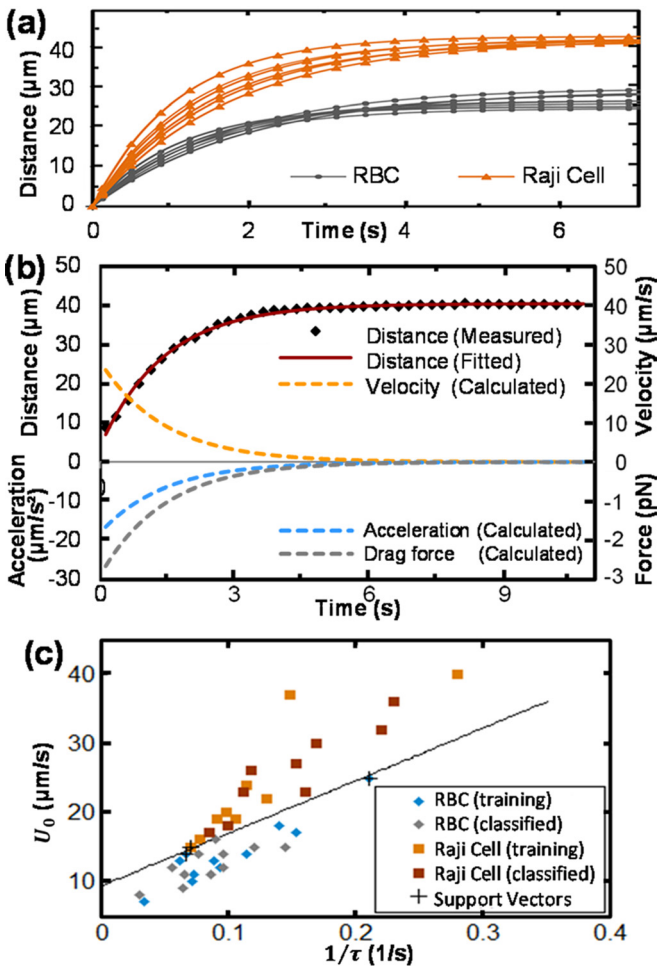

FIG. 4. (a) The relationship between distance and time for RBCs and Raji cells. (b) The variation of distance, velocity, acceleration and drag force with respect to time, respectively. (c) Classification of cells using a SVM algorithm.

is possible to distinguish between these different types of cells based on their motion under DEP. The experiment data are classified using a support vector machine (SVM)[14] algorithm. This is a supervised learning model with associated learning algorithms that analyzes data and recognizes patterns. SVM is commonly used for classification and regression analysis. The correct rate of classification in our experiment is 97.5%. Therefore, these results validate the feasibility of using the motion analysis for automatic differentiation among different types of cells.

This Letter proposes an improved theoretical model for the motion of a cell under the influence of DEP force. Based on the trajectory tracking of various types of human cells, we measured cell displacement as a function of time and calculated the associated velocities and accelerations. The experimental data matched well with the proposed theoretical model. Then, we analyzed the motion of the cells and distinguished between different types of cells based on their transient motion response under a specific DEP force field. The computer-vision based cell motion analysis described in this Letter using an ODEP system could be used to track cell motion trajectory accurately, while enabling the simultaneous identification and sorting of different types of cells. It is envisioned that this method could be further developed into non-invasive approaches to identify and differentiate cells, as well as quantify the dielectric properties of cells.

The authors would like to thank the financial supports from the Hong Kong Research Grants Council (Project Nos. 118513 and 125513) and the Chinese Academy of Sciences - Croucher Funding Scheme for Joint Laboratories (Project No. 9500011).

[1]P. Y. Chiou, A. T. Ohta, and M. C. Wu, Nature **436**, 370 (2005).
[2]W. Wang, Y.-H. Lin, T.-C. Wen, T.-F. Guo, and G.-B. Lee, Appl. Phys. Lett. **96**, 113302 (2010).
[3]W. Liang, N. Liu, Z. Dong, L. Liu, J. D. Mai, G.-B. Lee, and W. J. Li, Sens. Actuators, A **193**, 103 (2013).
[4]N. G. Green, A. Ramos, and H. Morgan, J. Electrost. **56**, 235 (2002).
[5]T. Sun, N. G. Green, and H. Morgan, Appl. Phys. Lett. **92**, 173901 (2008).
[6]S. L. Neale, A. T. Ohta, H.-Y. Hsu, J. K. Valley, A. Jamshidi, and M. C. Wu, Opt. Express **17**, 5232 (2009).
[7]S. L. Neale, M. Mazilu, J. I. B. Wilson, K. Dholakia, and T. F. Krauss, Opt. Express **15**, 12619 (2007).
[8]N. G. Green, A. Ramos, and H. Morgan, J. Phy. D: Appl. Phys. **33**, 632 (2000).
[9]Y. Huang, R. Hölzel, R. Pethig, and X. B. Wang, Phys. Med. Biol. **37**, 1499 (1992).
[10]J.-E. Kim and C.-S. Han, Nanotechnology **16**, 2245 (2005).
[11]A. Ramos, H. Morgan, N. G. Green, and A. Castellanos, J. Phys. D: Appl. Phys. **31**, 2338 (1998).
[12]G. Zhang, M. Ouyang, J. Mai, W. J. Li, and W. K. Liu, J. Lab. Autom. **18**, 161 (2013).
[13]M. L. Turgeon, *Clinical Hematology: Theory and Procedures*, 4th ed. (Lippincott Williams & Wilkins, Philadelphia, 2005), p. 100.
[14]J. A. K. Suykens and J. Vandewalle, Neural Process. Lett. **9**, 293 (1999).